Chirality

Deutsche Ausgabe: DOI: 10.1002/ange.201603771
Internationale Ausgabe: DOI: 10.1002/anie.201603771

The Interplay Between Conformation and Absolute Configuration in Chiral Electron Dynamics of Small Diols

*Steven Daly, Maurice Tia, Gustavo A. Garcia, Laurent Nahon, and Ivan Powis**

Abstract: *A competition between chiral characteristics alternatively attributable to either conformation or to absolute configuration is identified. Circular dichroism associated with photoexcitation of the outer orbital of configurational enantiomers of 1,3- and 2,3-butanediols has been examined with a focus on the large changes in electron chiral asymmetry produced by different molecular conformations. Experimental gas-phase measurements offer support for the theoretical modeling of this chiroptical effect. A surprising prediction is that a conformationally produced pseudo-enantiomerism in 1,3-butanediol generates a chiral response in the frontier electron dynamics that outweighs the influence of the permanent configurational handedness established at the asymmetrically substituted carbon. Induced conformation, and specifically induced conformational chirality, may thus be a dominating factor in chiral molecular recognition in such systems.*

Concepts describing molecular shape lie at the heart of much intuitive thinking about chemical reaction and interaction, from the simplest nucleophilic substitution processes to more complex enzyme interactions. Central to such considerations is the role of molecular chirality and consequent specificity of chiral recognition. Because macro-biomolecules tend to be chiral and built from smaller chiral units, an appreciation of how chiral information transfers at the molecular level assumes a wide-ranging significance for understanding the mechanisms of asymmetric synthesis. This includes the building up of supramolecular chirality and the many enantioselective processes of life (such as odor perception or pharmaceutical action). The commonest source of molecular chirality is, of course, an asymmetrically substituted carbon, which is a configurational chirality that could be considered to be hard-wired into the molecule. Among other sources of chirality, molecular handedness arising from a particular conformation is also possible. Chiral induction, the process whereby a static chirality can be induced in a prochiral or transiently chiral species by interaction with a moiety of specific chirality, without a requirement for bond-breaking, is a central topic in this context.[1–3] Relatively weak intermolecular forces, such as H-bonding, are often then implicated in the chirality transmission mechanisms; gas-phase studies, which remove a multitude of fluctuating solvent interactions of comparable energy that might obscure the intrinsic effect, have an important role to play.[4]

Herein we examine chirality using photoelectron circular dichroism (PECD). A particular advantage over other chiroptical measures is that PECD provides an orbitally selective probe of molecular chirality,[5–7] allowing specific focus to be given to responses of the HOMO frontier orbital. Specifically, PECD isolates and extracts the phenomenological coefficient, $b_1^{\{+1\}}$, of an odd $\cos\theta$ term in the photoelectron angular distribution (Supporting Information and Refs. [5,6]), which can then directly express the chiral asymmetry observed in the forward–backward ($\theta = 0,\ \pi$) directions as a Kuhn asymmetry factor, $g = 2\,b_1^{\{+1\}}$. From a theoretical perspective for interpretation, the $b_1^{\{+1\}}$ parameter embodies the dynamics of the mobile electron[5] as it is ejected from the selected orbital and moves out through the chiral potential of the molecular framework.

The small diols we consider herein, namely 1,3-propanediol (13PD), 1,3*R*-butanediol (13BD), and 2*R*,3*R*-butanediol (23BD), are flexible molecules with rotation around various bonds providing numerous possible conformations, but the energetically most favorable are significantly stabilized by the formation of intramolecular H-bonds. The two most stable conformers calculated for 13PD[8,9] and those calculated for 13BD are compared in Figure 1.[10,11] The four-letter designations used (*g′GG′t* and *tGG′g*) describe the four dihedral angles defining the structures; for brevity we also show and will use an alternative Roman numeral numbering.

These two most stable 13PD conformers can be seen to constitute an enantiomeric pair, related by the hindered rotation of the OH groups. However, as in many such conformational enantiomers, these chiral structures rapidly interconvert. In 13PD the relevant tunneling frequency is found to be 5.42 MHz,[9] and consequently its chirality is transient. Nevertheless, it is interesting to examine the instantaneous chirality. Theoretical calculations for the HOMO photoionization are presented in Figure 2. In particular we discuss here the non-zero chiral $b_1^{\{+1\}}$ parameter values that appear in the lower panel. Just as for any chiroptical asymmetry, exchanging the enantiomers (here conformers) flips the sign of $b_1^{\{+1\}}$. The (transient) conforma-

[*] Dr. S. Daly, Prof. Dr. I. Powis
School of Chemistry, University Park, University of Nottingham
Nottingham NG7 2RD (UK)
E-mail: ivan.powis@nottingham.ac.uk
Dr. S. Daly, Dr. M. Tia, Dr. G. A. Garcia, Dr. L. Nahon
Synchrotron SOLEIL, l'Orme des Merisiers
Saint Aubin BP 48, 91192 Gif sur Yvette Cedex (France)
Dr. S. Daly
Current address: Institut Lumiere Matière, UMR5306, CNRS,
Université Lyon 1, 69622 Villeurbanne (France)
Dr. M. Tia
Current address: Institut für Kernphysik
Johann Wolfgang Goethe Universität
Max-von-Laue-Strasse 1, 60438 Frankfurt am Main (Germany)
Supporting information and the ORCID identification number(s) for the author(s) of this article can be found under http://dx.doi.org/10.1002/anie.201603771.

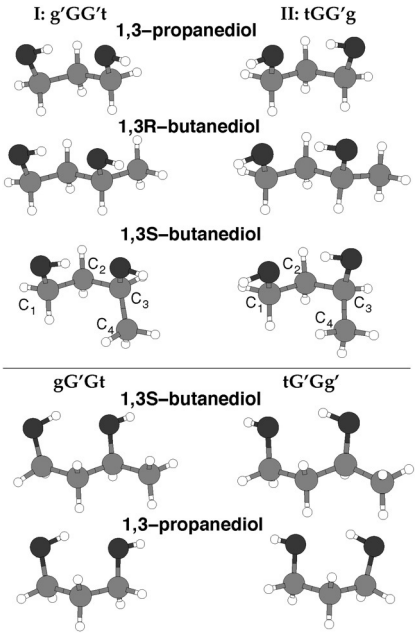

Figure 1. A comparison of the lowest-energy conformers (**I**, **II**) of 1,3-propanediol and 1,3*R*-butanediol. The alternative 1,3*S*-butanediol configuration, but retaining the same carbon C1–C3 conformations, appears in the third row, while true enantiomers of **I** and **II** appear in the bottom rows.

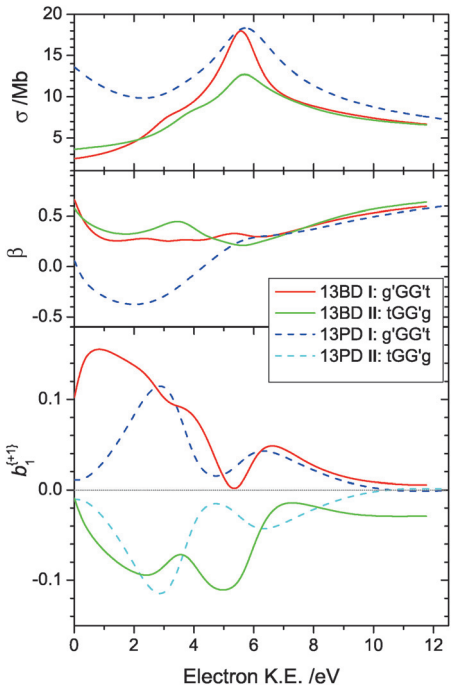

Figure 2. Calculated photoionization cross-section σ, anisotropy parameter β, and chiral $b_1^{\{+1\}}$ parameter for the HOMO of the 1,3*R*-butanediol quasi-degenerate conformers **I** and **II** (solid lines) compared with corresponding conformers of 1,3- propanediol (dashed lines). For σ and β the two 1,3-propanediol conformers (conformational enantiomers) provide indistinguishable results, and thus only one is plotted.

tional enantiomerism of 13PD is thus seen in the exact mirroring of the calculated $b_1^{\{+1\}}$ curves shown for this molecule.

It can be expected that methyl group substitution at the C3 atom in 13PD, to form 13BD, will effectively quench the tunneling identified in 13PD by destroying the C1:C3 equivalence and, consequently, the symmetric double-well inversion potential.[12] This is fully corroborated by the observation of uncoupled asymmetric top spectra for the **I** and **II** pair of 13BD, indicating their existence as distinct conformers.[10,11] But such addition of a methyl group also creates an asymmetric substitution at the C3 site, so generating permanent configurational enantiomerism in 13BD, with separable *R*,*S* enantiomers. Nevertheless, as can be seen in Figure 2, the calculated HOMO ionization cross-section and the anisotropy parameter β (both enantiomer-independent properties) retain many similarities to those for 13PD. More remarkably, the chirally sensitive $b_1^{\{+1\}}$ parameter curves for the two most stable 13BD conformers **I** and **II** also still approximate the chiral mirroring seen for the analogous conformers of 13PD, albeit for a fixed choice (*R*) of the 13BD configurational enantiomer. The strong visual similarities between the low energy structures of 13PD and 13BD (Figure 1) and between their $b_1^{\{+1\}}$ parameter curves (Figure 2) suggests some residual conformational enantiomerism in 13BD such that, for fixed absolute configuration, conformers **I** and **II** effectively constitute a pseudo-enantiomeric pair. An entirely analogous argument could be developed for the 3*S* configuration and its corresponding conformers.

This suggested pseudo-enantiomerism is further underscored by examining 13PD and 13BD HOMO orbital isosurface visualizations (Figure 3). Because of the strongly localized HOMO character, the (pseudo) enantiomerism is seen to be equally imprinted on the HOMO orbitals of both 13PD and 13BD in a manner that is not encountered with other more delocalized valence orbitals.

Before further discussing 13BD we turn to an examination of its isomer, 2,3-butanediol. A computational investigation of the conformer space of 23BD has been previously reported by Jesus et al.[13] The three most stable 2R,3R conformers (designated[13] **I**, **II**, **III**) are shown in Figure 4. These are estimated to jointly account for 90% of the room temperature

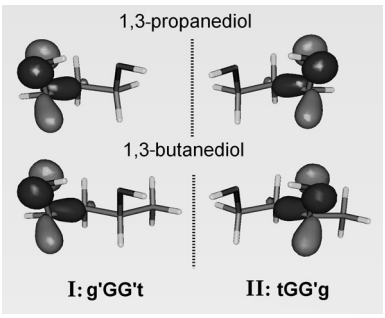

Figure 3. Hartree–Fock HOMO orbitals for conformers **I**, **II** of a) 1,3-propanediol and b) 1,3*R*-butanediol.

population, and more than 99% at 100 K. Our own calculations, summarized in the Supporting Information, Table S1, replicate the energetics reported previously.[13,14] Experimentally, a molecular beam Fourier-transform microwave spectroscopy study[14] has unambiguously identified conformer **I** as the dominant species present in jet-cooled conditions. Employing a similar cold molecular beam for an experimental PECD measurement we therefore have the opportunity to examine, effectively, a single isomer conformer.

Jet-cooled experimental results showing mean HOMO electron PECD values for 2*R*,3*R*-butanediol, recorded at various photon excitation energies, are presented in Figure 5 along with calculated $b_1^{\{+1\}}$ parameter curves for single conformers **I**–**III** and for an assumed 100 K conformer population average. Good agreement with the calculated PECD for the most stable conformer **I** is demonstrated, while significant contributions (more than the 15% expected for a 100 K Boltzmann distribution) from conformers **II** and **III** can be discounted, corroborating previous experiments.[14]

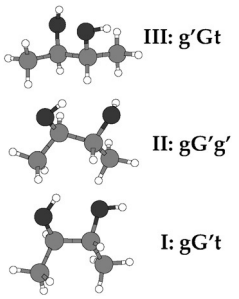

Figure 4. Lowest-energy conformers of 2*R*,3*R*-butanediol. **I** is most stable by at least 1.4 kJ mol^{-1}.

Having thus validated the theoretical method applied herein to study the HOMO PECD of single conformers of the butanediols, we return to the explicit consideration of 13BD. Our calculated properties for the quasi-degenerate conformers **I** and **II** and for the next most stable conformer, **III**, which is more than 2 kJ mol^{-1} higher in energy, are summarized in the Supporting Information, Table S2. FTIR measurements[10] on an annealed, cold 10 K matrix-isolated 13BD showed that the population collapsed to a 1:1 mix of the two thermodynamically most stable conformers. Correspondingly, an equally weighted preponderance of conformers **I** and **II** was inferred in a pulsed-jet FT microwave experiment.[11] It can thus be expected that under the cold molecular beam conditions of our PECD experiment, an approximately 1:1 mixture of conformers **I** and **II** will be obtained.

The lower panel of Figure 5 compares the predicted PECD for 13(*R*) BD conformers **I**–**III** and experiment. Individually, none of the 13BD conformers provides a good match with the jet-cooled experimental data. In particular, the magnitude of the experimental $b_1^{\{+1\}}$ parameters is less than that of the calculated single-conformer PECD curves. However, the anticipated 1:1 average of the conformer **I** and **II** $b_1^{\{+1\}}$ parameters provides significantly better agreement with experiment and we may infer that it is the approximate mutual cancellation (that is, the pseudo-enantiomerism) of this conformer pair that is responsible for an apparent attenuation of the PECD observed experimentally.

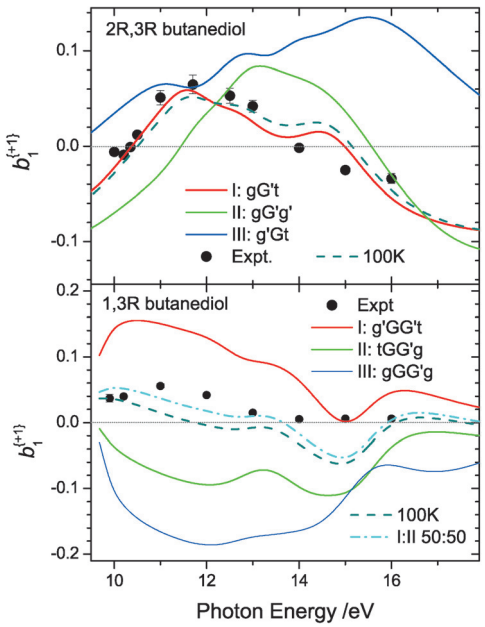

Figure 5. HOMO electron chiral $b_1^{\{+1\}}$ parameters for 2*R*,3*R*-butanediol (top) and 1,3*R*-butanediol (bottom). Calculations made at fixed equilibrium geometry for the low energy conformers **I**–**III** are shown as solid curves. 100 K Boltzmann population weighted averages (calculated using data from the Supporting Information, Tables S1, S2) and, for 13BD, a 1:1 mean of conformers **I** and **II** appear as broken lines. Jet-cooled experimental values, formed as averages taken across the HOMO band profile at each photon energy, are included for comparison; the error bars indicate uncertainty owing to the counting statistics.

It is well-established that PECD measurements are sensitive to absolute configuration at one or more stereogenic centers.[6] Although not included herein, repeating the above calculations for true enantiomers of the various conformations (for example, 13(*R*)-BD g′GG′t→13(*S*)-BD gG′Gt; see Figure 1) negates all the $b_1^{\{+1\}}$ parameter curves shown, and creates a clear disparity with the experimental data. Nevertheless, the calculated PECD curves for the chosen *R* enantiomer configurations of these butanediols (Figure 5) display a striking variation with assumed conformation, a sensitivity which is fully anticipated from previous PECD studies,[6] including cases where, as here, such large differences were ascribed simply to the rotational orientation of an OH group.[15,16] Equally, structural isomers such as camphor and fenchone can display very different PECD response even when sharing the same absolute configuration.[17] In these senses the various differences between 13BD and 23BD seen here are not unexpected. Perhaps more surprising are the highlighted similarities between 13PD and 13BD.

This pseudo-enantiomeric mirroring for 13BD **I** and **II** does, however, disappear at photon energies around 15 eV, nor does the experimental datum fit the calculated 1:1 mean PECD at this energy (Figure 5). A full analysis of the calculations indicates this region corresponds to a shape resonance in the electron continuum.[18] Here, it suffices to note that such resonances correspond to a temporary trapping of the photoelectron in the molecular vicinity. This allows the outgoing electron, which here we have seen is initially OH localized, an extended coupling to the entire molecular structure including assumedly the asymmetrically substituted C3 chiral center. The chiral electron dynamics observed in PECD generally derive from both the initial state (orbital), and a final state scattering of the outgoing electron off the

chiral molecular potential.[5] A reasonable inference is that in the 13BD calculated PECD conformation-induced pseudo-enantiomerism of the initially highly localized HOMO provokes the dominant sensed chirality but that this is effectively suppressed by an enhanced influence of configurational chirality at energies around the shape resonance. At the same time fixed geometry calculations such as these are known to overemphasize such resonant effects.[18]

Overall, notwithstanding the $h\nu \approx 15$ eV region of shape resonance, there is a clear implication that the conformers **I** and **II** of a given absolute configuration of 13BD constitute a pseudo-enantiomeric pair in which the terminal methyl group, despite strictly breaking mirror symmetry at the asymmetric C3 substitution site (hence leading to *R* or *S* absolute configurations), is a quasi-spectator. This therefore mimics the 13PD situation. Evidently this conformational pseudo-enantiomerism impacts the chirally sensitive HOMO PECD to an extent at least comparable to the absolute configurational chirality, leading to the approximate mirroring in the inferred HOMO electron dynamics.

Significantly, these findings illustrate that the effective chirality of even a relatively small molecule can be determined by its localized electronic structure, rather than the overall geometric arrangement of atoms, which is what most definitions of molecular chirality reference. While it can be argued that orbital chirality must ultimately follow from a chiral framework, this evidently need not span the whole molecule. In probing such localized electronic structure, PECD is perhaps closer than more traditional chiroptical methods (such as solution-phase electronic absorption CD) to the many chemical processes that interrogate molecular chirality via localized electronic interactions. As the orbital-specific response revealed herein demonstrates, this may entail some quite subtle considerations and consequently may be an important concept for understanding how chirality operates in macromolecular systems built up from smaller chiral units.

The quasi-degeneracy, and non-separability, of such isolated conformational enantiomers could be readily lifted in a molecular recognition event. Imprinting of chiral information through relatively weak molecular interactions (such as the formation and disruption of H-bonds, and any consequent modification of frontier orbital response) assumes a wide-ranging significance for understanding the many enantioselective processes encountered in life. The involvement of such interactions in any chiral recognition processes with 13BD is clearly sufficient to induce different pseudo-enantiomeric conformations. Although the single photon PECD technique as applied here offers no time resolution, the new ultrafast laser based variants of PECD that are emerging[19–21] offer a clear prospect of performing time-resolved pump-probe PECD measurements capable of following the interconversion of conformers, and any associated chiral switching, in real time.[6,7]

Experimental Section

Experiments were performed at the Soleil synchrotron on the DESIRS beamline.[22] An imaging photoionization spectrometer equipped with a skimmed supersonic molecular beam source was employed to measure photoelectron angular distributions for alternating left and right circularly polarized vacuum ultraviolet radiation, with $b_1^{\{+1\}}$ values extracted following a general methodology described previously.[23] Calculations of the chiral photoionization dynamics used the CMS-Xα method. More specific details on both experiment and calculation are provided in the Supporting Information.

Acknowledgements

We thank the general staff of SOLEIL and particularly J.-F. Gil, for his technical help on the DESIRS beamline under proposal no. 20110312, funded from the European Community's Seventh Framework Program (FP7/2007–2013) under Grant Agreement No. 226716. Use of the EPSRC UK National Service for Computational Chemistry Software (NSCCS) is gratefully acknowledged (Projects CHEM559 and CHEM720).

Keywords: absolute configuration · chirality · circular dichroism · 1,3-propanediol

How to cite: *Angew. Chem. Int. Ed.* **2016**, *55*, 11054–11058
Angew. Chem. **2016**, *128*, 11220–11224

[1] A. Zehnacker, M. A. Suhm, *Angew. Chem. Int. Ed.* **2008**, *47*, 6970; *Angew. Chem.* **2008**, *120*, 7076.
[2] G. A. Hembury, V. V. Borovkov, Y. Inoue, *Chem. Rev.* **2008**, *108*, 1.
[3] J. Thomas, W. Jager, Y. Xu, *Angew. Chem. Int. Ed.* **2014**, *53*, 7277; *Angew. Chem.* **2014**, *126*, 7405.
[4] A. Zehnacker, *Chiral Recognition in the Gas Phase*, Taylor & Francis, Boca Raton, **2010**.
[5] I. Powis in *Advances in Chemical Physics*, *Vol. 138* (Ed.: J. C. Light), Wiley, New York, **2008**, p. 267.
[6] L. Nahon, G. A. Garcia, I. Powis, *J. Electron Spectrosc. Relat. Phenom.* **2015**, *204*, 322.
[7] M. H. M. Janssen, I. Powis, *Phys. Chem. Chem. Phys.* **2014**, *16*, 856.
[8] S. Vázquez, R. A. Mosquera, M. A. Rios, C. Vanalsenoy, *J. Mol. Struct. THEOCHEM* **1988**, *50*, 149.
[9] D. F. Plusquellic, F. J. Lovas, B. H. Pate, J. L. Neill, M. T. Muckle, A. J. Remijan, *J. Phys. Chem. A* **2009**, *113*, 12911.
[10] M. T. S. Rosado, A. J. L. Jesus, I. D. Reva, R. Fausto, J. S. Redinha, *J. Phys. Chem. A* **2009**, *113*, 7499.
[11] B. Velino, L. B. Favero, A. Maris, W. Caminati, *J. Phys. Chem. A* **2011**, *115*, 9585.
[12] S. L. Baughcum, R. W. Duerst, W. F. Rowe, Z. Smith, E. B. Wilson, *J. Am. Chem. Soc.* **1981**, *103*, 6296.
[13] A. J. L. Jesus, M. T. S. Rosado, I. Reva, R. Fausto, M. E. Eusebio, J. S. Redinha, *J. Phys. Chem. A* **2006**, *110*, 4169.
[14] J. Paul, I. Hearn, B. J. Howard, *Mol. Phys.* **2007**, *105*, 825.
[15] G. A. Garcia, H. Soldi-Lose, L. Nahon, I. Powis, *J. Phys. Chem. A* **2010**, *114*, 847.
[16] G. A. Garcia, L. Nahon, C. J. Harding, I. Powis, *Phys. Chem. Chem. Phys.* **2008**, *10*, 1628.
[17] L. Nahon, L. Nag, G. A. Garcia, I. Myrgorodska, U. Meierhenrich, S. Beaulieu, V. Wanie, V. Blanchet, R. Géneaux, I. Powis, *Phys. Chem. Chem. Phys.* **2016**, *18*, 12696.
[18] J. L. Dehmer, D. Dill, A. C. Parr in *Photophysics and Photochemistry in the Vacuum Ultraviolet* (Eds.: S. P. McGlynn, G. L. Findley, R. H. Huebner), D. Reidel, Dordrecht, **1985**, p. 341.

[19] C. Lux, M. Wollenhaupt, T. Bolze, Q. Q. Liang, J. Kohler, C. Sarpe, T. Baumert, *Angew. Chem. Int. Ed.* **2012**, *51*, 5001; *Angew. Chem.* **2012**, *124*, 5086.
[20] C. S. Lehmann, N. B. Ram, I. Powis, M. H. M. Janssen, *J. Chem. Phys.* **2013**, *139*, 234307.
[21] A. Ferré, C. Handschin, M. Dumergue, F. Burgy, A. Comby, D. Descamps, B. Fabre, G. A. Garcia, R. Géneaux, L. Merceron, E. Mével, L. Nahon, S. Petit, B. Pons, D. Staedter, S. Weber, T. Ruchon, V. Blanchet, Y. Mairesse, *Nat. Photonics* **2015**, *9*, 93.
[22] L. Nahon, N. D. Oliveira, G. Garcia, J. F. Gil, B. Pilette, O. Marcouille, B. Lagarde, F. Polack, *J. Synchrotron Radiat.* **2012**, *19*, 508.
[23] L. Nahon, G. A. Garcia, C. J. Harding, E. A. Mikajlo, I. Powis, *J. Chem. Phys.* **2006**, *125*, 114309.

Received: April 19, 2016
Revised: May 21, 2016
Published online: July 22, 2016

